

Chicago, Chicago, Ill.

¹N. F. Mott and H. S. W. Massey, *The Theory of Atomic Collisions* (Clarendon, Oxford, 1965), especially p. 530

²See Refs. 5 and 19.

³See Refs. 6, 15, and 16.

⁴Y. Hahn, T. F. O'Malley, and L. Spruch, *Phys. Rev.* **128**, 932 (1962); *Phys. Rev.* **130**, 381 (1963); M. Gailitis, *Zh. Eksp. Teor. Fiz.* **47**, 160 (1964) [*Soviet Physics-JETP* **20**, 107 (1965)].

⁵C. Schwartz, *Phys. Rev.* **124**, 1468 (1961); R. L. Armstead, University of California Laboratory Report No. -11628, 1964 (unpublished); see also Ref. 15.

⁶See Refs. 8, 10, 14, 16, 19, and 20.

⁷P. G. Burke and A. J. Taylor, *J. Phys. B* **2**, 869 (1969); A. L. Sinfailam and R. K. Nesbet, *Phys. Rev. A* **6**, 2118 (1972).

⁸P. G. Burke and H. M. Schey, *Phys. Rev.* **126**, 147 (1962); K. Smith and L. A. Morgan, *Phys. Rev.* **165**, 110 (1968); see also Ref. 18.

⁹W. A. McKinley and J. H. Macek, *Phys. Letters* **10**, 210 (1964); see also Refs. 4 and 14.

¹⁰P. G. Burke, D. F. Gallaher, and S. Geltman,

J. Phys. B **2**, 1142 (1969).

¹¹R. J. Damburg and E. Karule, *Proc. Phys. Soc.* **90**, 637 (1967).

¹²M. J. Seaton, *Comments At. Molec. Phys.* **1**, 184 (1970).

¹³R. S. Ruffine, New York University Research Report No. CX-48, 1960 (unpublished).

¹⁴J. F. Perkins, *Phys. Rev.* **173**, 170 (1968).

¹⁵P. G. Burke and A. J. Taylor, *Proc. Phys. Soc.* **88**, 549 (1966).

¹⁶M. Gailitis, in *Physics of Electronic and Atomic Collisions* (Science Bookcrafters, Hastings-on-Hudson, N. Y., 1965), p. 10.

¹⁷M. E. Rose, *Elementary Theory of Angular Momentum* (Wiley, New York, 1957).

¹⁸I. C. Percival and M. J. Seaton, *Proc. Camb. Phil. Soc.* **53**, 654 (1957); R. Marriot, *Proc. Phys. Soc.* **72**, 121 (1958).

¹⁹K. T. Chung and J. C. Y. Chen, *Phys. Rev. A* **6**, 686 (1972).

²⁰I. Aronson, Y. Hahn, P. M. Henry, C. J. Kleinman, and L. Spruch, *Phys. Rev.* **153**, 73 (1967).

PHYSICAL REVIEW A

VOLUME 7, NUMBER 6

JUNE 1973

Cross Sections for *K*-Shell Ionization by 2-MeV-Electron Impact

Angela Li-Scholz

*Department of Physics, State University of New York at Albany,
and State University of New York, Empire State College, Albany, New York 12206*

R. Collé* and I. L. Preiss

Department of Chemistry, Rensselaer Polytechnic Institute,† Troy, New York 12181

W. Scholz

*Department of Physics, State University of New York at Albany, Albany, New York 12222
(Received 16 February 1973)*

A systematic study of the cross sections for *K*-shell ionization by 2.0-MeV-electron impact has been made as a function of atomic number. The cross sections for 32 elements from V ($Z=23$) to Bi ($Z=83$) were first measured relative to each other, and then were normalized to 43 b at Sn ($Z=50$). Thus systematic errors usually associated with absolute measurements were minimized and did not obscure minor variations in the Z dependence of the cross sections. The measured values drop from 353 b at V to 9.9 b at Bi. The general trend of the Z dependence of the data is in agreement with theoretical predictions of Kolbenstvedt. However, variations in cross sections by as much as 30% from one element to the next are not accounted for by the theory.

I. INTRODUCTION

The subject of inner-shell ionization by relativistic electrons has not been studied in any great detail either theoretically or experimentally. This is evidenced by both the lack of rigorous relativistic calculations for *K*-shell ionization and the sparsity of cross-section measurements. Specifically, *K*-shell ionization cross sections have been measured for only seven elements in the MeV energy range, and most of these measurements were at or below 2 MeV.¹⁻⁴ A series of experiments has also been performed in the extreme relativistic

range of electron energies from 150 to 900 MeV, in which *K*-shell ionization cross sections were measured for eight elements ranging from Cu to Bi.⁵ Within the experimental error limits of these measurements, the dependence of the *K*-shell ionization cross section on the electron energy has been found to be a smooth function. This feature is in agreement with the predictions of all existing theoretical approaches.⁶⁻⁸

Theoretical treatments of *K*-shell ionization by electrons are in the majority of cases completely nonrelativistic⁹ and hence not applicable to the present experiment. In the work of Arthurs and

Moiseiwitsch⁶ relativistic effects for the incident electron have been included. Using Darwin wave functions for the bound electron, they performed a calculation which they assert is applicable for atoms with atomic numbers $Z < 30$ and for electron impact energies less than 22 times the K -shell ionization potential of the relevant atom. A calculation that uses Dirac wave functions for both the incident and the bound electron has been made by Perlman⁷ for Hg. The only theoretical treatment that appears to be applicable for the entire periodic range of elements and for electron energies up to 900 MeV has been given by Kolbenstvedt.⁸ In his work, the K -shell ionization cross section has been derived using the method of virtual photons combined with the photoelectric cross section for distant collisions. For close collisions, the impulse approximation in conjunction with the Møller formula for free-electron scattering has been used to calculate their contribution to the cross section.

In presenting his theoretical treatment, Kolbenstvedt⁸ reviewed the then existing experimental data for relativistic incident electrons and compared them with his own and other applicable theories. Except for the experimental results of Ref. 2, the various theories agree with each other and with the experimental data to within about 25%. However, for comparison with theory beyond a statement of approximate agreement, more data are clearly required. In this paper, we will present the full details of K -shell ionization cross-section measurements at 2.0-MeV incident electron energy for 32 elements, ranging from V ($Z = 23$) to Bi ($Z = 83$). A brief account of this work has been reported previously.¹⁰

II. EXPERIMENTAL

A. Procedure

The measurement of relative K -shell ionization cross sections was based on the determination of relative $K\alpha$ x-ray yields. Thin targets were fabricated which contained a well-determined ratio of atoms of element Z to Cd. As a target was irradiated by 2-MeV electrons, the fluorescent x rays were detected in lithium-drifted Si or Ge counters. Typical spectra measured with the Si (Li) and the Ge (Li) detector system, respectively, are shown in Figs. 1(a) and 1(b). To deduce the relative $K\alpha$ x-ray yield of element Z to Cd from the observed spectrum, it is sufficient to know only the Z/Cd atom ratio and the relative efficiency of the detector at the appropriate $K\alpha$ x-ray energies. This procedure obviates the necessity of determining the electron beam intensity, the absolute number of target atoms, the precise solid angle, or the absolute detector efficiency. The choice of Cd as the reference element was somewhat arbitrary. It was considered a good choice because its $K\alpha$ x-ray

energy of 23 keV is high enough not to be easily absorbed, but still low enough to be easily detected. In addition, Cd is readily available, inexpensive, and has convenient chemical properties.

B. Setup

The 4-MeV Dynamitron accelerator at the State University of New York at Albany was used to accelerate the electrons. The high voltage of the accelerator was set and stabilized via a resistive feedback system. The high-voltage control helipot was calibrated with the ${}^9\text{Be}(\gamma, n)$ reaction which has a threshold of 1.66510 ± 0.00037 MeV.¹¹ Bremsstrahlung was produced by stopping the electron beam in a 120-mg/cm² gold foil backed with graphite. Immediately behind the graphite was a 3-mm stack of Be foils. A BF_3 counter was used to observe the onset of neutron production as the high-voltage settings were varied. In these measurements, the accuracy with which the threshold could be defined was found to be better than 0.5%. However, because of a nonlinear behavior of the high-voltage control circuit, the precision was

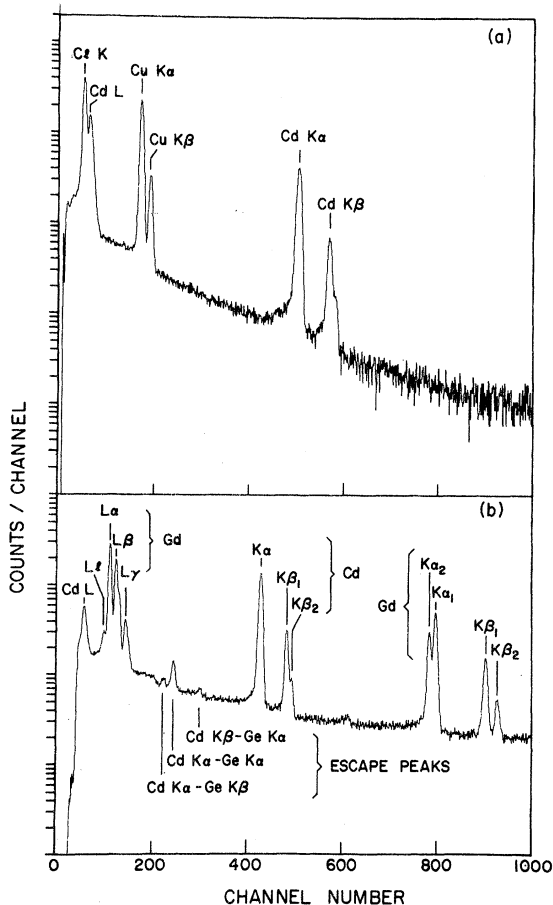


FIG. 1. Typical x-ray spectra obtained with (a) the Si(Li) detector and (b) the Ge(Li) detector.

actually somewhat less at other voltages.

The electron beam was focused and steered to the target position by electrostatic and magnetic deflection through a series of apertures on the 0° beam line. Successive sections of beam pipes on the line were electrically isolated such that, by monitoring the current readings on the sections before and behind the target, the extent of the scattering of the beam by the target could be ascertained. For the present experiments, the portion of beam scattered in the backward direction was never in excess of 1%.

A schematic drawing of the experimental layout is shown in Fig. 2. The gate valve served to separate the target chamber section from the accelerator when opening up to air for target changes. The beam was positioned by focusing through a 1-cm-diam aperture located 30 cm upstream from the target. Proper centering of the beam must be checked in the vicinity of the target, because the earth's magnetic field is sufficient to cause the electron beam to be deflected through an arc as it proceeds down the 4-in. beam pipe. Once the beam was positioned, the aperture was removed before starting the x-ray measurements in order to avoid x-ray production in the target by bremsstrahlung background. The target was mounted with its normal at 45° with respect to the direction of the incident electron beam. After traversing the target the electrons entered a 250-cm-long section of beam pipe, which served as a beam dump and Faraday cup.

The measurements of impact ionization cross sections reported in this paper were performed at 2.00 ± 0.05 MeV. Typically, the average electron current was 50 nA over approximately a 2-cm² area of the target.

C. Detectors

Two series of measurements were made using a Si(Li) and a Ge(Li) detector, respectively. The Si(Li) detector had a 0.025-mm-thick Be entrance window. This detector was directly coupled to the vacuum of the target chamber through a gate valve and was located 51.5 cm from the center of the target. The Ge(Li) detector had a 0.13-mm-thick Be window and a 40.4- $\mu\text{g}/\text{cm}^2$ Au layer evaporated onto its front face. X rays detected with this system emerged from the target chamber through a 0.051-mm-thick Mylar window of 2.54 cm in diameter. The air path between this exit window and the entrance window of the Ge(Li) detector was 38.6 cm. Both detectors were placed at 90° with respect to the direction of the incident electron beam.

The detector, Si(Li) or Ge(Li), was shielded against scattered electrons and bremsstrahlung. To attenuate the bremsstrahlung arising from

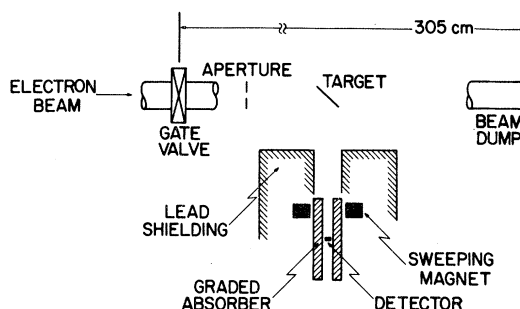


FIG. 2. Schematic of the experimental arrangement.

electrons striking the beam pipe, the detector assembly was shielded from all sides by 5–10 cm of lead, except for a 4-cm-diam opening in the direction of the incident x rays. Further degradation of the secondary radiation was effected by covering all surfaces in the line of sight of the detector with a graded absorber of plastic, aluminum, and copper. To sweep away scattered electrons, a 1000-G permanent magnet was placed in front of the detector. The magnet itself was encased in a plastic mold with a 4-cm-diam hole between the pole pieces.

The energy resolution values reported by the manufacturers were 216 eV at 6.4 keV for the Si(Li) system and 177 eV at 5.9 keV for the Ge(Li) system. Under the actual experimental conditions of this work, however, the resolution at 6.4 keV was close to 300 eV for both detectors. No great effort was made to optimize the resolution, since the K x-ray signatures were generally well above background. According to the manufacturer's specifications, the sensitive regions were 4 mm in diameter by 3 mm thick for the Si(Li) detector, and 6 mm in diameter by 4.79 mm thick for the Ge(Li) detector. Measurements made of the absolute and relative efficiencies of the detectors showed that both detectors were smaller than specified. A brief description of the efficiency calibration procedure is given below.

The relative efficiencies as a function of energy are primarily determined by the thickness of the detector. Israel, Lier, and Storm¹² compared photopeak efficiency calculations using Monte Carlo methods and using the exponential absorption law for a 0.3-cm-thick Si(Li) detector and for a 0.7-cm-thick Ge(Li) detector. Below 60 keV for the Si(Li) detector and below 100 keV for the Ge(Li) detector, the efficiency ϵ calculated by the Monte Carlo method was very well reproduced by

$$\epsilon = 1 - e^{-(\mu/\rho)x}, \quad (1a)$$

where (μ/ρ) is the energy absorption coefficient¹³ and x is the detector thickness. At energies above 60 keV, the Monte Carlo calculation showed that

the Si(Li) detector efficiency continues to drop off exponentially. The slope of the drop is the same as that calculated from the expression

$$\epsilon = 1 - e^{-(\mu/\rho)_{\text{ph}}x}, \quad (1b)$$

where $(\mu/\rho)_{\text{ph}}$ is the photoelectric mass absorption coefficient.¹³ In the present measurements, the Si(Li) detector was used for $K\alpha$ x rays up to the 52 keV (Yb) and the Ge(Li) detector to 76 keV (Bi). Therefore, in both cases, Eq. (1a) should give a proper representation of the efficiency as a function of energy. Where the calculation was extended to higher energies for purposes of testing detector thicknesses, the findings of the above-cited paper¹² were used as a guide. It can be noted, incidentally, that the divergences between the Monte Carlo and the exponential-law calculations arise out of multiple processes the magnitude of whose effect increases with detector thickness. As will be demonstrated presently, the detectors used for these experiments are substantially thinner than those in Ref. 12 and hence the corresponding divergences should be even less pronounced.

In the calibration of the Si(Li) detector, a thin source of ^{57}Co was used for the determination of the relative efficiencies at 14.4, 122, and 136 keV (open circles in Fig. 3). The relative γ -ray intensities were taken from the average of the results of several recent reports.¹⁴ Comparison of the measured and calculated relative efficiencies indicated that the thickness of the detector was ~ 1.7 mm. Three additional measurements were made of absolute efficiencies at 60, 88, and 122 keV, using ^{241}Am , ^{109}Cd , and ^{57}Co (closed circles in Fig. 3). These absolute efficiency measurements were made by comparison to a standard 3×3 -in. NaI(Tl) detector using the NaI(Tl) efficiency calculations of Heath.¹⁵

Assuming the diameter of the Si(Li) detector to be 4 mm as specified by the manufacturer, the intrinsic efficiencies deduced from these measurements were found to fit very well with the curve calculated for 1.7 mm (see Fig. 3). The experimental uncertainties associated with these absolute efficiencies were in all cases $< 10\%$. Since the relative intensities of the ^{57}Co γ rays are very well known, the corresponding relative efficiencies are also well determined and have uncertainties which are small compared to 10% . Even assuming an uncertainty of 10% for each of the points at 60, 88, and 122 keV, the detector thickness would nevertheless be confined to values between 1.5 and 1.9 mm. For the analysis of the relative cross-section data, the efficiency ratios $\epsilon_{K\alpha}(Z)/\epsilon_{K\alpha}(\text{Cd})$ used were taken from the curve calculated for 1.7 mm. The differences between these numbers and the corresponding ones for 1.5 and 1.9 mm were assigned as possible errors on the $\epsilon_{K\alpha}(Z)/$

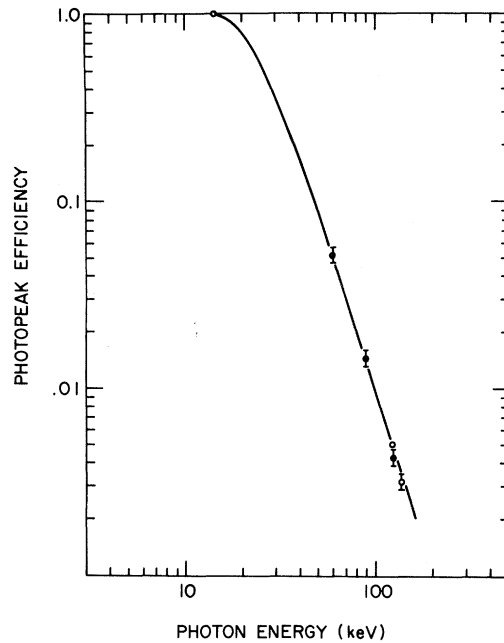


FIG. 3. Photopeak efficiency of the Si(Li) detector as a function of photon energy. The solid curve is that calculated for 1.7-mm thickness. The measured points were obtained with ^{57}Co , ^{109}Cd , and ^{241}Am sources. For details see text.

$\epsilon_{K\alpha}(\text{Cd})$ values. Obviously, such differences would be largest for elements whose atomic numbers are very different from 48 (Cd). In no case, however, is the difference greater than 8% .

By performing similar calibration measurements, the thickness of the Ge(Li) detector was found to be about 3.5 mm. In order to account both for the manufacturer's claim of a thickness of 4.79 mm and for the apparent measured thickness of 3.5 mm, we adopted a value of 4.0 ± 1.0 mm for the data analysis. It should be noted that x rays below 50 keV are nearly totally absorbed by 3 mm of Ge. Therefore, this rather large uncertainty in the thickness affects only the very high- Z elements to any appreciable degree. The maximum associated error in the efficiency is that for the 76-keV $K\alpha$ x ray of Bi, which is of the order of 10% . The Ge(Li) detector was not used for the low- Z region because of the large absorption effects associated with its thicker Be window and with the air path between target and detector.

In calculating the photopeak efficiency for the Ge(Li) detector, the effect of escape peak losses was included. The ratios of escape to photopeak intensity were taken from a smooth curve drawn through the experimental points of Palms, Venugopala Rao, and Wood.¹⁶ A 30% uncertainty was assumed for these ratios to account for the spread in the data. For the Si(Li) detector calculation, escape losses

were neglected since the magnitude of the effect is < 1% even for the lowest-energy x ray (4.95 keV for V) measured in this experiment.

D. Targets

In preparing targets for the present experiments, several requirements were considered. The targets should be thin in order to minimize (i) the degradation of the electron beam energy and intensity, (ii) the production of bremsstrahlung, and (iii) self-absorption of the x rays. At the same time, the target must contain a very precisely known ratio of atoms of element Z to atoms of Cd. Simplicity of preparation was also deemed an important criterion since a large number of targets covering a wide range of Z values was desired.

The general method employed consisted of preparing solutions with known Z /Cd atom ratios, dipping thin lens tissues into these solutions, and then air drying the lens papers. The lens tissue used was Fisher No. 11-996 which has an average thickness of 1.35 mg/cm². The additional target material of Cd and element Z absorbed was typically 1 mg/cm². The solutions were prepared by mixing together and dissolving known weights of Cd and element Z . The chemicals used were generally of reagent-grade quality. The weights were measured with a Mettler single-pan analytical balance and have an accuracy of about ± 0.2 mg. Since most solutions were prepared using 10 mmole of each element in principle the atom ratios Z /Cd were determined to better than 0.5%. The complete dissolution of the two components is, however, an indispensable requirement. Moreover, the purity and the physical and chemical properties of the materials used must be considered to ensure a proper correlation between the weight of the substance and the number of atoms. For example, a particular hydrated compound may be unsuitable because the number of waters of hydration changes with atmospheric conditions.

Crucial to this target preparation procedure is the requirement that the final atom ratios in the targets be identical to those deduced from the weights of the initial components. To verify that this requirement was satisfied, three series of tests were conducted. In the first, targets were made from sample solutions having a wide range of solution concentrations and atom ratios. These targets and sample solutions were then independently chemically analyzed. The determinations were made by atomic absorption and emission flame photometry using standard procedures.¹⁷ For the starting sample solutions, analyses were made on aliquot parts of the same solutions used to prepare the targets. The targets themselves were assayed by taking a known area of the target, digesting it in nitric acid, and extracting a known

aliquot part of the liquid for the analyses. The results of these measurements for Cu/Cd, Ag/Cd, La/Cd, Gd/Cd, and Pb/Cd targets are shown in Table I. As indicated, the atom ratios obtained from the sample solutions and from the target assays are in good agreement with those calculated from the sample weights. The observed small discrepancies of a few percent are believed to primarily reflect the precision of the chemical assays.

In the second series of tests, several targets selected from among those actually used for the cross section measurements were assayed. The resultant atom ratios from the assays and those obtained from the sample weights are given in Table II. As before, only several percent differences in the atom ratios were found and they again mainly reflect the precision of the chemical analyses.

The purpose of the third series was to test whether variations in the chemical composition of the targets or the amount of target material had any effect on the outcome of the results. Several

TABLE I. Comparison of atom ratios for successive steps of the target preparation procedure: (a) calculated from the weights of the starting chemical reagents; (b) obtained from chemical analyses of the sample solutions; (c) obtained from chemical analyses of the lens tissue targets.

Z /Cd target	Molarity Cd in solution	atom ratio, a_Z/a_{Cd}		
		(a)	(b)	(c)
Cu/Cd	0.50	0.934	0.951	0.942
	0.25	0.934	0.936	0.897
	0.10	0.934	0.925	0.940
	0.50	0.0979	0.0980	0.0963
	0.25	0.0979	0.0947	0.0955
	0.10	0.0979	0.0964	0.0977
	0.50	0.0138	0.0133	0.0142
	0.25	0.0138	0.0137	0.0129
	0.10	0.0138	0.0128	0.0137
Ag/Cd	0.50	2.148	2.183	2.137
	0.50	0.965	1.005	0.984
	0.10	0.965	0.973	0.991
	1.00	0.517	0.507	0.513
La/Cd	0.50	1.011	1.008	1.015
	0.10	1.011	1.019	1.002
	0.05	1.011	0.997	1.006
	1.00	0.493	0.494	0.488
	0.20	0.493	0.490	0.493
	0.10	0.493	0.477	0.485
Gd/Cd	0.25	2.024	2.057	2.034
	0.05	2.024	2.036	2.002
	0.25	1.106	1.105	1.133
	0.05	1.106	1.009	1.110
Pb/Cd	0.25	2.005	2.018	2.026
	0.05	2.005	1.984	2.004
	0.25	0.197	0.195	0.193
	0.05	0.197	0.197	0.196

TABLE II. Comparison of atom ratios for several targets which were actually used for the cross-section measurements.

Z/Cd target	atom ratio, a_Z/a_{Cd}	
	From sample weights ^a	From target assay ^a
Ag/Cd	0.9754	0.957
Ba/Cd	0.7469	0.765
La/Cd	1.0592	1.003
Ce/Cd	0.9026	0.918
Gd/Cd	1.9247	1.880

^aSee Table I for explanation.

targets each of Pr/Cd, Nd/Cd, Eu/Cd, and Gd/Cd were made in which the atom ratios, sample solution concentrations and the solvents used for dissolving the reagents were varied. By utilizing hydrochloric acid, nitric acid, and aqua regia as the dissolving solvents, targets were obtained in which the target elements were deposited as different compounds (e. g., chlorides or nitrates). For all these cases, the atom ratios in the targets reproduced those expected from sample weights to within a few percent.

E. Target Corrections

For an incident electron energy of 2 MeV, a ~ 2.5 -mg/cm²-thick target positioned at 45° with respect to the incident electron beam can be considered as thin. The average energy loss for the electron is only about 7 keV and the amount of bremsstrahlung produced is not serious (see Appendix A). By a simple order-of-magnitude calculation, it can also be shown that the excitation of one element by the K x ray of the other amounts to less than 2% of the K-shell ionization events for the most unfavorable case studied. For low-energy x rays, however, self-absorption in the target may be nontrivial. To derive the proper correction factors for this effect, a series of x-ray attenuation measurements were made using the experimental arrangement shown in the inset in Fig. 4. X rays were produced by fluorescing a thin target (A) of the desired element Z. The intensity of x rays arriving at the detector was measured with and without an interposed lens tissue Z/Cd target (B), thereby determining an effective attenuation factor $e^{-\eta t}$. Uniformity of the target thickness was checked by performing the transmission measurements on different areas of the absorber. No discernible differences were found in any of the cases that were investigated.

Having obtained ηt , the fractional target transmission T , defined as the ratio of the intensities of x rays emerging from the target to the total

x rays produced, could then be calculated for the particular geometry of a target placed at 45° to both the electron beam and the detector. The values of T , given by

$$T = (\cos 45^\circ / \eta t) [1 - \exp(-\eta t / \cos 45^\circ)] \quad (2)$$

as a function of Z that were thus obtained are shown in Fig. 4. The maximum deviation of any measured point from the smooth curve drawn is less than 2%. The regularity of the curve is presumably due to the similarity of the targets. That is, they all had a Z/Cd atom ratio of about unity and the lens tissue appears to absorb a rather uniform amount of material of approximately 1 mg/cm² in all cases.

III. RESULTS AND DISCUSSION

The measured $K\alpha$ x-ray intensities were first corrected for self-absorption in the target and for absorption in the windows between the target and the detector. No corrections were made for the angular dependence of the emitted x rays, which has been found to be isotropic.^{1,5} From the corrected relative $K\alpha$ x-ray intensities, the $K\alpha$ x-ray production cross section $\sigma_{K\alpha}$ was derived using

$$\sigma_{K\alpha} = NI/\epsilon, \quad (3)$$

where the quantities I and ϵ are, respectively, the relative $K\alpha$ x-ray intensity and the relative detector efficiency at the $K\alpha$ x-ray energy. The quantity N is the proportionality constant which normalizes our relative measurements to $\sigma_{K\alpha} = 30.24$ b at Sn ($Z = 50$). The latter value was derived from the experimental K -shell ionization cross section of 44 ± 4 b, measured at 2.00-MeV incident energy, by dividing out the fluorescence yield value of 0.84

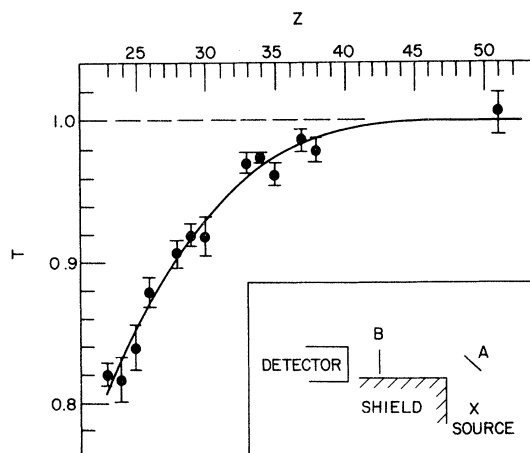


FIG. 4. Fractional transmission T for the $K\alpha$ x rays of element Z in the Z/Cd targets. The experimental arrangement used for the measurements is shown in the inset.

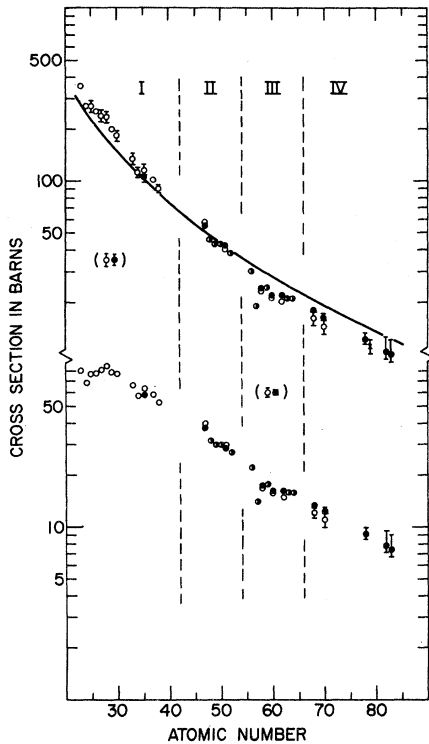


FIG. 5. K -shell ionization cross sections (upper) and $K\alpha$ x-ray production cross sections (lower) as a function of atomic number for 2.0-MeV incident electron energy. The data are normalized to $\sigma_K = 43$ b at Sn ($Z = 50$). The open and closed circles correspond, respectively, to measurements with the Si(Li) and Ge(Li) detector systems. The half-filled circles represent data points where the overlap of the two sets is better than 2%. The solid curve is that calculated from the Kolbenstvedt (Ref. 8) theory. The value for Au indicated by a cross is taken from Ref. 3. See text for a discussion of the normalization and the error bars.

used in Ref. 3 and accounting for the $K\beta/K\alpha$ transition probability ratio.¹⁸

From the $K\alpha$ x-ray production cross sections, K -shell ionization cross sections were derived according to the following relationship:

$$\sigma_K = \sigma_{K\alpha} [1 + P(K\beta)/P(K\alpha)]/\omega_K. \quad (4)$$

The values of the K -shell fluorescence yield needed for Eq. (4) were taken from Ref. 19, using what are referred to as "fitted values." The uncertainty in ω_K , given as "total uncertainty $\Delta\omega_K$ " in Ref. 19, is propagated as an error in the present analysis.²⁰ Values of the radiative transition probability ratios $P(K\beta)/P(K\alpha)$ were taken from Ref. 18. Errors in σ_K arising from uncertainties in this ratio amounted to less than 1%. In using these values of ω_K and $P(K\beta)/P(K\alpha)$, it is implicitly assumed that multiple inner-shell ionization does not occur to any appreciable extent. From such studies as Refs. 21 and 22, this assumption appears to be

justified for the range of elements studied in the present investigation.

The results for the $K\alpha$ x-ray production cross section (lower) and the K -shell ionization cross section (upper) are shown in Fig. 5. The open and closed circles represent, respectively, data obtained with the Si(Li) and Ge(Li) detection systems. The half-filled circles represent those cases where the overlap in the two sets of data is better than 2%. The measurement of Rester and Dance³ for Au at 2 MeV is also shown and is indicated by a cross. The error bars on the data points include uncertainties in counting statistics, background subtraction, and absorption of the x rays either in the target or in other materials. For the K -shell ionization cross sections, errors in the fluorescence yields are also included. The absence of an error bar implies that the uncertainty is less than 5%. With the exception of region IV ($Z > 66$), however, the error bars do not include any contribution from the efficiency calibration of the two detectors. The approximate efficiency calibration uncertainties appropriate to the regions I and III are depicted in Fig. 5 by the error bars on the points enclosed in parentheses, those for region II being too small to show on this scale. In region IV the photopeak efficiency of the Si(Li) detector has dropped off to the point where appreciable statistical uncertainty was becoming evident. For the Ge(Li)-detector data points, the main source of error is the uncertainty in the detection efficiency itself. Efficiency calibration uncertainties are included in the error bars shown for region IV, in addition to the errors previously enumerated. Since the errors in the efficiency calibration are primarily due to uncertainties in the detector thicknesses, these errors are correlated such that the upper error limit in region I corresponds to the lower limit in regions III and IV and vice versa. Within each of the first three regions, however, the relative errors in the data points arising from detection efficiency uncertainties are very minor. Also not shown is a systematic error of $\pm 9\%$ on all cross sections resulting from the uncertainty of ± 4 b in the absolute K -shell ionization cross section for Sn as given in Ref. 3. The effect of such an error would only be to move the entire set of data up or down.

The most surprising result of the present measurements is the observation of local irregularities in the Z dependence in the $K\alpha$ x-ray production cross sections. That is, sudden drops in the cross section are observed after V ($Z = 23$), As ($Z = 33$), Ag ($Z = 47$), and Ba ($Z = 56$). Because of the errors associated with ω_K , the corresponding structures in the K -shell ionization cross section appear somewhat less prominent. The pronounced drop of 30% in the cross sections at La ($Z = 57$) is most apparent.

As shown in Fig. 5, the results obtained with both detectors indicate an abrupt change in the slope of the data in this region. This phenomenon is especially surprising since all of the succeeding elements are also rare earths with very similar physical and chemical properties. Because of the unexpected nature of these fluctuations, it may be useful to recapitulate the considerations of possible systematic errors: (a) The effects of photon (bremsstrahlung and x-ray) induced ionization was shown to be negligible. (b) x-ray self-absorption in the targets did not indicate any evidence for Z -dependent selective attenuation. (c) Errors in the detector efficiencies can not produce local fluctuations. (d) The target-preparation procedure was checked to verify that the atom ratios in the lens tissue targets reproduced those of the sample solutions. This reproduction was found to be independent of the amount of target material or the chemical form of the target elements.

The Kolbenstvedt⁸ theory is the only existing theoretical treatment for K -shell ionization by relativistic electrons that is applicable to the present data. This theory predicts a smooth variation of the cross section as a function of atomic number. The curve drawn in Fig. 5 has been calculated using the simple analytical formula derived by Kolbenstvedt. Although the local variations in the experimental K -shell ionization cross sections are not accounted for by the theory, the general trend of the theoretical prediction follows the experimental data rather well. In the medium- Z region ($Z \sim 50$), the agreement is excellent, but the predicted cross sections are systematically too small in the low- Z region ($Z \lesssim 40$) and too large in the high- Z region ($Z \gtrsim 60$). This deviation in the heavy elements was also indicated by the measurements for gold by Rester and Dance³ at 2.0 MeV, and by Berkner *et al.*⁴ at energies of 2.5 and 7.1 MeV. No previous data are available for comparison in the light elements. If allowance is made for possible errors due to the efficiency calibration in our measurements, then these systematic deviations may not necessarily be significant. Nevertheless, the observed localized fluctuations would still exist and would remain to be explained by theory.

ACKNOWLEDGMENT

We wish to thank the staff of the Nuclear Accelerator Laboratory at the State University of New York at Albany for their assistance in carrying out this work.

APPENDIX A

The calculation which follows demonstrates that bremsstrahlung does not contribute importantly to K -shell ionization in the target.

The targets used in the present experiments all

measured about 1 mg/cm², exclusive of the weight of the lens tissue. Since the 1 mg/cm² consists of compounds of Cd and of elements Z , probably not more than 0.5 mg/cm² is actually elements Cd and Z , with the remainder consisting of elements H, O, Cl, etc. The thickness of the lens tissue backing is approximately 1.35 mg/cm². For the sake of simplicity, let the following approximate description be adopted for all targets: 1.0 mg/cm² to consist of Cd and element Z with an atom ratio of 1:1 and 2.5 mg/cm² of C. These weights should also adequately account for the additional thickness due to the target being at 45° to the incident electron beam direction.

For a target of atomic number Z , the differential cross section $d\sigma_{\text{rad}}$ for bremsstrahlung in the energy range between $h\nu$ and $h\nu + d(h\nu)$ from incident electrons of kinetic energy T is given by²³

$$d\sigma_{\text{rad}} = \sigma_0 B Z^2 [(T + m_0 c^2)/T] [d(h\nu)/h\nu], \quad (5)$$

where

$$\sigma_0 = \frac{1}{137} (e^2/m_0 c^2) = 0.580 \text{ mb/nucleus}$$

and B is a slowly varying function of Z and T , of the order of magnitude of 10.

The number of quanta produced per electron is, therefore,

$$dN_Q = d\sigma_{\text{rad}} n t, \quad (6)$$

where n and t are the number of atoms/g and the number of g/cm², respectively. The number²⁴ of these quanta which would be absorbed in the full thickness of the target via the photoelectric effect is

$$dN_Q (1 - e^{-n\tau t}) \simeq dN_Q n\tau t, \quad (7)$$

where

$$\tau \simeq p Z^4 / (h\nu)^3 \quad (8)$$

is the photoelectric cross section and $p \simeq 4 \times 10^{-32}$ cm² MeV³ (Ref. 23). The number of bremsstrahlung produced K -shell holes is therefore

$$N_b = \int_{I_K}^{h\nu \text{ max}} dN_Q n\tau t, \quad (9)$$

where the lower limit of integration I_K is the K -shell ionization potential.

In the present three-component target system, each of the three elements can give rise to bremsstrahlung, and each element can be ionized by the bremsstrahlung due to itself or the other two elements. Putting into Eq. (9) the quantities appropriate to any given pair of elements, carrying out the integration and neglecting the contribution from the upper limit, the K -shell holes in element 1 due to bremsstrahlung produced by element 2 is

$$N_b(1, 2) = n_1 t_1 n_2 t_2 Z_1^4 Z_2^2 \sigma_0 B p [(T + m_0 c^2)/T] (1/3I_1^3). \quad (10)$$

Since

$$N_b(1, 2)/N_b(1, 1) = n_2 t_2 Z_2^2 / n_1 t_1 Z_1^2, \quad (11)$$

the total number of *K*-shell holes in element 1 of the three elemental system is

$$\begin{aligned} N_b(1) &= N_b(1, 1) + N_b(1, 2) + N_b(1, 3) \\ &= N_b(1, 1) \left(1 + \frac{n_2 t_2 Z_2^2}{n_1 t_1 Z_1^2} + \frac{n_3 t_3 Z_3^2}{n_1 t_1 Z_1^2} \right). \quad (12) \end{aligned}$$

To ascertain the importance of the effect of bremsstrahlung in the present experiment, the number $N_b(1)$ must be compared to $N_e(1) = n_1 t_1 \sigma_K(1)$, which is the number of *K*-shell holes produced by direct electron ionization. The ratios N_b/N_e calculated for the *Z*/Cd targets used in the experiments ranged typically from 0.8 to 1.2%. Corrections to the cross sections due to the bremsstrahlung effect were neglected in the analysis.

*Present address: Department of Chemistry, Brookhaven National Laboratory, Upton, N. Y. 11973.

†Work supported in part by the U.S. Atomic Energy Commission.

¹J. W. Motz and R. C. Placious, *Phys. Rev.* **136**, A662 (1964).

²H. Hansen, H. Weigmann, and A. Flammersfeld, *Nucl. Phys.* **58**, 241 (1964).

³D. H. Rester and W. E. Dance, *Phys. Rev.* **152**, 1 (1966).

⁴K. H. Berkner, S. N. Kaplan, and R. V. Pyle, *Bull. Amer. Phys. Soc.* **15**, 786 (1970).

⁵L. M. Middleman, R. L. Ford, and R. Hofstadter, *Phys. Rev. A* **2**, 1429 (1970).

⁶A. M. Arthurs and B. L. Moiseiwitsch, *Proc. Roy. Soc. (London)* **A247**, 550 (1958).

⁷H. S. Perlman, *Proc. Phys. Soc. (London)* **76**, 623 (1960).

⁸H. Kolbenstvedt, *J. Appl. Phys.* **38**, 4785 (1967).

⁹See, for example, H. S. W. Massey, E. H. S. Burhop, and H. B. Gilbody, *Electronic and Ionic Impact Phenomena* (Oxford U.P., Oxford, England, 1969), Vol. I; N. F. Mott and H. S. W. Massey, *The Theory of Atomic Collisions*, 3rd ed. (Oxford U.P., Oxford, England, 1965); B. L. Moiseiwitsch and S. J. Smith, *Rev. Mod. Phys.* **40**, 238 (1968), and references quoted therein.

¹⁰W. Scholz, Angela Li-Scholz, R. Collé, and I. L. Preiss, *Phys. Rev. Lett.* **29**, 761 (1972).

¹¹A. H. Wapstra and N. B. Gove, *Nucl. Data* **A9**, 303 (1971).

¹²H. I. Israel, D. W. Lier, and E. Storm, *Nucl. Instrum. Methods* **91**, 141 (1971).

¹³E. Storm and H. I. Israel, *Nucl. Data* **A7**, 565 (1970).

¹⁴J. L. Campbell, P. O'Brien, and L. A. McNelles, *Nucl. Instrum. Methods* **92**, 269 (1971).

¹⁵R. L. Heath, AEC Research and Development Report No. IDO-16880-1, Physics, TID-4500 Vol. 1, 1964 (unpublished).

¹⁶J. M. Palms, P. Venugopala Rao, and R. E. Wood, *Nucl. Instrum. Methods* **64**, 310 (1968).

¹⁷Perkin-Elmer Corp., Publication No. 990-9638 (1968) (unpublished); R. Mavrodineanu and H. Boiteux, *Flame Spectroscopy* (Wiley, New York, 1965).

¹⁸G. C. Nelson, B. G. Saunders, and S. I. Salem, *At. Data* **1**, 377 (1970).

¹⁹W. Bambynek, B. Crasemann, R. W. Fink, H. U. Freund, H. Mark, C. D. Swift, R. E. Price, and P. Venugopala Rao, *Rev. Mod. Phys.* **44**, 716 (1972).

²⁰The fluorescence yield for Sn (*Z*=50) given in Ref. 19 is $\omega_K = 0.859$, as opposed to the value of 0.84 used in Ref. 3. This normalizes our values for the *K*-shell ionization cross sections to 43 b at Sn (instead of 44 b as given in Ref. 3).

²¹T. A. Carlson, W. E. Moddeman, and M. O. Krause, *Phys. Rev. A* **1**, 1406 (1970).

²²V. P. Sachenko and E. V. Burtsev, *Izv. Akad. Nauk. SSSR, Ser. Fiz.* **31**, 965 (1967) [*Bull. Acad. Sci. USSR, Phys. Ser.* **31**, 980 (1968)].

²³R. D. Evans, *The Atomic Nucleus* (McGraw-Hill, New York, 1955), pp. 603 and 698.

²⁴This, of course, somewhat overestimates the true number of absorbed quanta, since not all the bremsstrahlung quanta traverse the entire thickness of the target.